ELSEVIER

www.elsevier.nl/locate/carres

Carbohydrate Research 318 (1999) 10–19

CARBOHYDRATE RESEARCH

Solvent-dependent conformational behaviour of lipochitoligosaccharides related to Nod factors

Leandro Gonzalez [a], Manuel Bernabe [a], Juan Felix Espinosa [a], Pilar Tejero-Mateo [b], Antonio Gil-Serrano [b], Natacha Mantegazza [c], Anne Imberty [c], Hugues Driguez [c], Jesus Jimenez-Barbero [a,*]

[a] *Instituto Quimica Orgánica, CSIC, Juan de la Cierva 3, E-28006 Madrid, Spain*
[b] *Departamento de Química Orgánica, Facultad de Química, Universidad de Sevilla, E-41071 Seville, Spain*
[c] *Centre de Recherches sur les Macromolécules Végétales, CERMAV-CNRS [1], BP 53, F-38041 Grenoble, France*

Received 17 November 1998; accepted 29 March 1999

Abstract

The solution conformation of two lipooligosaccharides related to Nod factors or lipochitoligosaccharides have been analysed by 1D and 2D ^{1}H and ^{13}C NMR spectroscopy, molecular mechanics and dynamics calculations. The obtained data indicate that the glycosidic torsion angles have restricted fluctuations, but may adopt a variety of shapes. Remarkably, the relative orientation of the fatty acid chain towards the oligosaccharide backbone is solvent dependent. In water solution, the acyl residue and the oligosaccharide adopt a quasi-parallel orientation for a significant amount of time.

Keywords: Conformational analysis; Nuclear magnetic resonance; Molecular dynamics; Nodulation factors

1. Introduction

Rhizobia are nitrogen-fixing bacteria that are able to invade the roots of leguminous plants and trigger the formation of nodules that contain the nitrogen-fixing microsymbiont. Infection and nodule development are highly specific and depend on both partners, the bacterium and the plant, to be effective. During the symbiotic process, the host plant roots secrete flavonoids that induce the rhizobial nodulation genes (*nod* and *nol* genes) [1–3]. These genes have been shown to be involved in the synthesis and excretion of bacterial nodulation signals called nodulation (Nod) factors or lipochitoligosaccharides (LCOs).

The Nod factors are oligosaccharides consisting of a backbone of three to five GlcNAc residues, bearing an amide-bound fatty acyl residue (saturated or unsaturated) on the non-reducing terminal glucosamine residue. This basic skeleton has structural variations that determine the host-specificity. Compounds with *O*-sulfate, *O*-carbamoylate, and *N*-methyl have been identified, and different studies have indicated a close relationship between host specificity and Nod factor structure, regardless of the taxonomy of the bacterial symbiont. Tetra- or pentasaccharides whose reducing ends are glycosylated at position O-6 by either α-fucosyl or 2-*O*-methyl-α-fucosyl residue have also been described. Recently, a structure that bears a fucosyl residue α-(1→3)-linked to the *N*-acetylglu-

* Corresponding author. Tel.: +34-91-562-2900; fax: +34-91-564-4853.

[1] Affiliated with J. Fourier University.

0008-6215/99/$ - see front matter
PII: S0008-6215(99)00082-8

cosaminyl residue proximal to the nonreducing terminal *N*-acetylglucosaminyl residue and a novel minimal structure having only a N,N^{II}-diacetyl-chitobiosyl backbone structure have been identified [4].

The amino group of the nonreducing end glucosaminyl residue is acylated with C-16 or C-18 fatty acid chains with one to four double bonds such as those of *cis*-vaccenic (C18:1). It is also usually N-methylated.

Thus, the host-specificities of *Rhizobium leguminosarum* bv. *viciae* and *trifolii* are determined by the lipid moiety [5]. The sulfate group on O-6 of the reducing glucosaminyl residue is necessary for nodulation by *Sinorhizobium meliloti* of alfalfa plants [6]. Finally, bacteria that are symbionts of soybean (*Bradirhizobium japonicun* and *Sinorhizobium fredii*) and the broad host-range *Rhizobium* sp. NGR234 produce nodulation factors that are 6-O-substituted on the reducing glucosaminyl residue with a 2-*O*-methyl fucosyl residue [1,7–10].

The structures of the LCOs produced by *Sinorhizobium fredii* HH103 have been reported [10] and shown to consist of a backbone of chitin oligomers ranging from trimer to pentamers, substituted by fucosyl (minor components) and 2-*O*-methyl fucosyl (major components) at the reducing terminal *N*-acetylglucosamine residue and N-acylated at the non-reducing terminal residue with octadecanoic acid, *cis*-octadec-11-enoic acid, *cis*-hexadec-9-enoic acid or hexadecanoic acid. Further studies have shown that the presence of 2-*O*-methyl-fucosyl in the LCOs produced by *S. fredii* strain HH103 is important for the efficiency of nodulation on some legumes as *Cajanus cajan* and for the bacterial competitive capacity to nodulate soybean.

The biological relevance of these molecules has encouraged several groups to perform structural studies of different Nod factors. Several reports on the synthesis of several LCOs and analogues have also been described [11]. In many examples, biological properties of molecules strongly depend on their conformation and their configuration. Amide Z/E isomerism due to hindered rotation has been studied in simple derivatives [12], but, to the best of our knowledge, no detailed conformational analysis on these molecules has been reported so far. The conformation of chitooligosaccharides has been studied in several instances, since chitobiose is a key component of the glycoprotein oligosaccharide chains. However, the relative orientation of the oligosaccharide and lipid chains is not precisely known, along with the extent of flexibility around the glycosidic linkages of the backbone and the pendant groups.

We report here on the conformational studies of two of these LCOs in solution, namely **1** and **2**, by using NMR and molecular mechanics and dynamics calculations (Fig. 1). These compounds have been isolated [10] and synthesized [13] in Seville and Grenoble, respectively. It is shown that the backbone displays a major conformation, similar to that described for regular chitooligosaccharides, but that the relative orientation of the fatty acid chain with respect to the backbone is solvent dependent. In particular, in water solution, the acyl chain spends a significant time adopting a quasi-parallel orientation to the oligosaccharide chain. In **1**, the 6-O-linked 2-*O*-methyl fucosyl residue may adopt a variety of conformations.

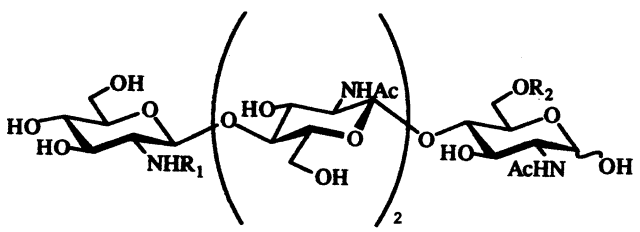

1, R_1= $COC_{17}H_{33}$ (10Z), R_2 = 2-O-Me-α-Fucopyranosyl
2, R_1= $COC_{15}H_{29}$ (9Z), R_2 = SO_3^-

Fig. 1. Schematic view of LCOs **1** and **2**.

2. Experimental

Molecular mechanics and dynamics calculations.—Molecular mechanics and dynamics calculations were performed using both the CVFF force field [14] within the INSIGHT II/DISCOVER programs of BIOSYM technologies (San Diego, CA, USA) and the MM3* force field as implemented in MACROMODEL 4.5 [15]. Φ is defined as H1′–C1′–O–C4 and Ψ as C1′–O–C4–H4. For the 6-O-linked 2-*O*-methyl fucose residue, Φ is defined as H1″–C1″–O6–C6 and Ψ as C1″–O6–C6–C5. Only the *gg* orienta-

tion of the lateral chain was used for the β-GlcNAc moieties of the backbone, except for the 6-O-substituted one. For the $1\rightarrow6$ linkage, both gg and gt rotamers [16] were considered for the β-glucosaminyl moiety. Separate calculations for a dielectric constant $\varepsilon = 80$ (with CVFF and MM3* for compound **1**) and for the continuum GB/SA solvent model (with MM3* for compound **2**) were performed [17]. First, potential-energy maps were calculated for the constituent disaccharide (*N*,*N*′-diacetyl chitobiose): relaxed (Φ,Ψ) potential-energy maps were calculated as described [18]. One intial geometry of the secondary hydroxyl groups of the pyranosyl moieties was considered, r (reverse clockwise). The previous step involved the generation of the corresponding rigid residue maps by using a grid step of 18°. Then, every Φ,Ψ point of this map was optimised using 200 steepest descent steps, followed by 1000 conjugate gradient iterations. From these relaxed maps, the probability distributions were calculated for each ϕ, ψ point according to a Boltzmann function at 303 K.

Starting structures of both oligosaccharides **1** and **2** were built by combining the more stable conformers of the different glycosidic linkages and subjecting them to extensive energy minimization with conjugate gradients. An extended structure of the acyl chain was used as input geometry. The sulfate group was employed in the MM3* simulations using the parameters developed by Perez [19]. Then, these structures were used as starting geometries for molecular dynamics (MD) simulations [20] at 300 K. The CVFF ($\varepsilon = 80$, compound **1**) and the MM3* force field ($\varepsilon = 80$, compound **1,** GB/SA, compound **2**) [17] were employed with a time step of 1 fs. The equilibration period was 100 ps. After this period, structures were saved every 0.5 ps. The total simulation time was between 2 and 3 ns for every run. Average distances between intra-residue and inter-residue proton pairs were calculated from the dynamics simulations.

NMR spectroscopy.—NMR experiments were recorded on a Varian Unity 500 spectrometer, using an approximately 3 mg mL^{-1} solution of the lipooligosaccharides at different temperatures. The spectra for lipopentasaccharide **1** were recorded in a 49:1 DMSO-d_6–D_2O solvent mixture, due to solubility problems in pure water. Those spectra for sulfated lipotetrasaccharide **2** were acquired in D_2O. Chemical shifts are reported in ppm, using the residual HDO signal (4.71 ppm) and external TMS (0 ppm) as references. The double quantum filtered COSY spectrum was performed with a data matrix of 256×1 K to digitize a spectral width of 2000 Hz. Sixteen scans were used with a relaxation delay of 1 s. The 2D TOCSY experiment was performed using a data matrix of 256×2 K to digitize a spectral width of 2000 Hz. Four scans were used per increment with a relaxation delay of 2 s. MLEV 17 was used for the 100 ms isotropic mixing time. The one-bond proton–carbon correlation experiment was collected using the gradient-enhanced HMQC sequence [21]. A data matrix of 256×2 K was used to digitize a spectral width of 2000 Hz in F_2 and 10,000 Hz in F_1. Four scans were used per increment with a relaxation delay of 1 s and a delay corresponding to a J value of 145 Hz. ^{13}C decoupling was achieved by the WALTZ scheme. The 2D-HMQC-TOCSY experiment was conducted with 80 ms of mixing time (MLEV 17). The same conditions as for the HMQC were employed. HMBC experiments were performed using the gradient enhanced sequence with a data matrix of 256×2 K to digitize a spectral width of $2000 \times 15{,}000$ Hz. Eight scans were acquired per increment with a delay of 65 ms for evolution of long range couplings.

2D NOESY, 2D ROESY, and 2D T-ROESY experiments were performed using four different mixing times, namely 150, 300, 450, and 600 ms, with 256×2 K matrices. Good linearity was observed up to 200 ms (NOESY) and 300 ms (ROESY). Estimated errors in the NOE intensities are smaller than 20%.

3. Results and discussion

Conformational analysis: molecular dynamics studies.—In a first step to determine the overall three-dimensional structure of the lipooligosaccharides, molecular mechanics and dynamics calculations were performed. Infor-

Table 1
Torsional angle values (Φ,Ψ) of the predicted minima and MM3* (GB/SA solvent model) and CVFF ($\varepsilon = 80$) populations of the low-energy regions of **1** and **2** [a]

	β(1→4) linkage			α(1→6) linkage
MM3*	A	B	C	A
Torsion angle (Φ/Ψ)	48/5	−40/173	175/−6	−52/−175
Population (%)	96.2	3.7	0.1	100.0
CVFF	A	B	C	A
Torsion angle (Φ/Ψ)	55/2	−52/−172	178/4	−58/−179
Population (%)	98.7	1.3	<0.1	100.0

[a] The regions around Φ extend ca. 25° and around Ψ ca. 35°.

mation on the accessible amount of conformational space was obtained through molecular dynamics simulations [20] of **1** and **2**. Simulations with the DISCOVER-CVFF and MM3* programmes were performed, since they have provided satisfactory results in the study of the conformation of a variety of oligosaccharide molecules [22]. For uncharged compound **1**, both force fields were shown to provide similar results as also described for smaller disaccharides [22f]. Simulations at a high dielectric constant were performed, according to our previous studies which demonstrated that for these two force fields there is a minor dependence of the results on the dielectric constant used [22f]. First, relaxed potential-energy maps (Φ/Ψ) were calculated for N,N^{II}-diacetyl-chitobiose [22e]. The glycosidic linkage presents well-defined low-energy regions, which cover less than 20% of the complete potential energy surface. All the energy regions show Φ values (Table 1) which are centred around those expected for the exo-anomeric effect [23], although the expected probability distributions occupy a wide surface. Then, two models of the pentasaccharide **1** were built, composed of all the different glycosidic linkages of the polysaccharide and the fatty acid chain, and submitted to different 2 or 3 ns simulations again using both force fields. Both gg and gt conformations of the lateral chain of the 2-*O*-methyl Fuc*p*-(1→6)-β-D-GlcNAc linkage were considered. For all linkages, the glycosidic torsion angles cover a well-defined part of the complete Φ/Ψ map, which is fairly independent of the rotamer present at the hydroxymethyl group of the reducing β-D-GlcNAc moiety. Independently of the force fields used, the glycosidic torsion angles Φ and Ψ show oscillations centred at 60 and 0° (Fig. 2). In all cases, these torsional oscillations are more pronounced around Ψ, as expected by the operativity of the exo-anomeric effect around Φ. Some excursions to the anti regions are evident. In terms of the available space for the interglycosidic torsion angles, the calculated results are fairly similar for the different β-(1→4)-linkages, almost independently of the particular structure of the

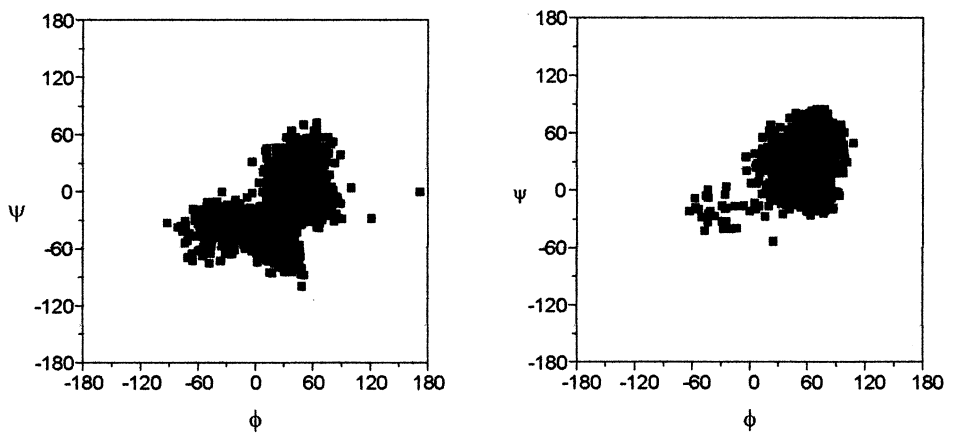

Fig. 2. Trajectory plots of the MD simulation (1 ns) of **1** by using MM3* ($\varepsilon = 80$). The trajectories of the simulation in Φ/Ψ space for two of the β(1→4) glycosidic linkages are shown. The trajectories of the β(1→4) glycosidic linkages during the CVFF ($\varepsilon = 80$) simulation of **1** and the MM3* (GB/SA) simulation of **2** are basically identical.

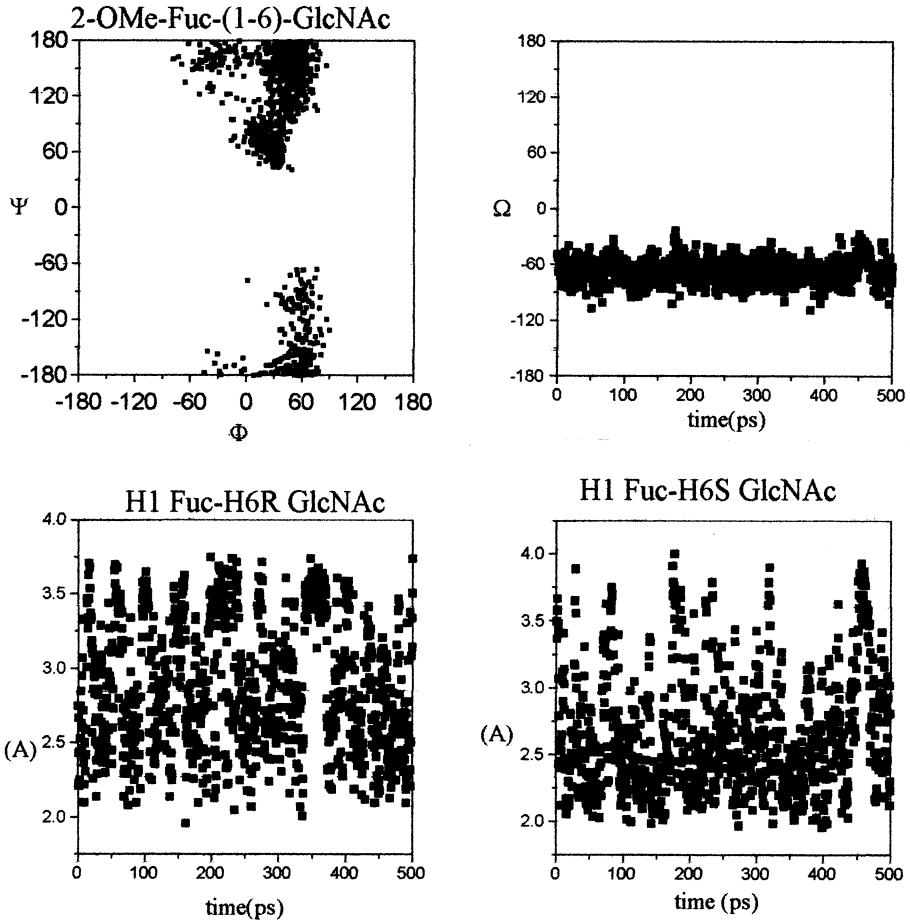

Fig. 3. Trajectory plots of the MD simulation (1 ns) of **1** by using MM3* ($\varepsilon = 80$). The relevant information for the fucose glycoside linkage is presented. The trajectory of this $\alpha(1\rightarrow6)$ glycosidic linkage during the CVFF ($\varepsilon = 80$) simulation is basically identical.

N-acyl moiety. For the Φ/Ψ values (Table 1) sampled during these trajectories, no important interaction of the Fuc moiety with the contiguous GlcNAc residue takes place. In fact, with respect to the accessible conformational space for the $(1\rightarrow6)$-linkage (Fig. 3), the observed results are also independent on the conformation (gg or gt) of the exocyclic chain and indicate a larger accessible area of conformational space. In most of the cases, several transitions between the rotamers of the hydroxymethyl group were observed. Nevertheless, the hydroxymethyl groups displayed either the gg or the gt conformations for most of the simulation time ($>90\%$) Finally, average expected interproton distances from the different MD simulations (Table 2) were estimated and compared to those observed experimentally. No close proton–proton distances were deduced from the MD models which

Table 2
Average relevant proton–proton inter-residue distances from the MM3* ($\varepsilon = 80$) MD simulations for **1** (starting from gg and gt conformers for the $\alpha(1\rightarrow6)$ linkage of **1**) and experimentally observed NOEs (strong (s), medium (m), weak (w)) [a]

	gg	gt	NOE intensity
AH1/BH6S	2.86	3.12	m
AH1/BH6R	2.47	2.37	s
CH1/BH4	2.36	2.38	s
CH1/BH6S	3.07	2.53	m
CH1/BH6R	2.53	2.90	m
DH1/CH4	2.43	2.36	s
DH1/CH6S	2.93	2.80	m
DH1/CH6R	3.36	3.00	m
EH1/DH4	2.45	2.39	s
EH1/DH6S	2.91	2.51	m
EH1/DH6S	3.35	2.92	m

[a] The average simulation results for both compounds are basically identical independently of the force field (MM3* or CVFF) and conditions ($\varepsilon = 80$ or GB/SA) used.

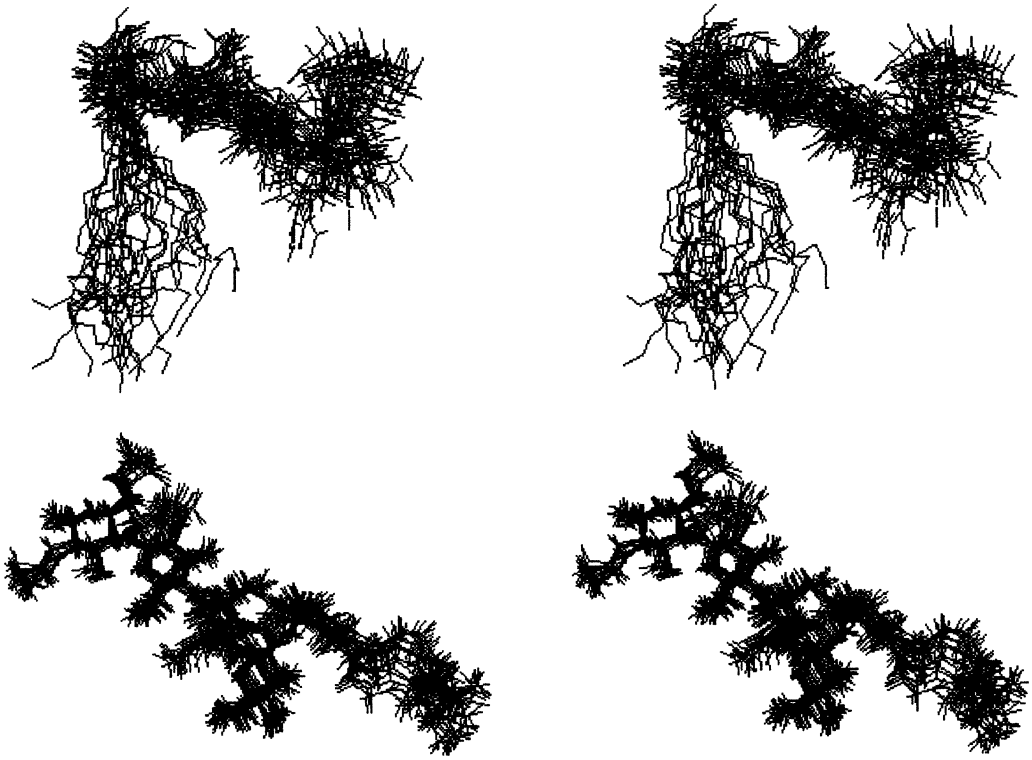

Fig. 4. Superimposition of several snapshots taken from the MD simulations of **1** (MM3*, $\varepsilon = 80$, bottom) and **2** (MM3*, GB/SA, top). The existence of an important amount of flexibility around the glycocidic linkages is evident.

were not apparent in the experimental NOE data.

A superimposition of different conformers found in the MD simulation is shown in Fig. 4. It is shown that despite the relatively narrow variation of the glycosidic torsion angles, the conformational space accessible to the lipid chain may be fairly large. Regarding the orientation of the lipid chain, it is observed that it may display a variety of orientation with respect to the sugar residues. In fact, for some time, it may remain in close contact with the sugar residues, adopting a quasi-parallel disposition with regard to the tetrasaccharide backbone, making van der Waals contacts below 3.7 Å.

Regarding the sulfated tetrasaccharide **2**, GB/SA simulations were carried out with the MM3* programme. Similar results were observed to those described above for **1**, both regarding the oligosaccharide backbone (Fig. 5) and the lateral chain. Thus, the obtained trajectories do not depend either on the size of the oligosaccharide or the nature of the acyl chain. A large variation on the orientation of the *O*-sulfate chain were observed. Nevertheless, for the Φ values (Table 1) sampled during the trajectory, which are those expected for the exo-anomeric effect, no important interaction of the sulfate group with the contiguous GlcNAc residue takes place. A superimposition of different conformers found in the MD simulation is shown in Fig. 6.

^1H NMR data.—Since NMR parameters are essentially time averaged, the information that it is possible to deduce from these experiments corresponds to the time-averaged conformation in solution. The validity of the theoretical results has been tested using NMR measurements of vicinal coupling constants and NOEs [24,25]. ^{1}H NMR and ^{13}C NMR spectra were completely assigned by a combination of homonuclear COSY, TOCSY, and heteronuclear HMQC, HMBC, and HMQC-TOCSY techniques. The corresponding ^{1}H and ^{13}C NMR chemical shifts are listed in Tables 3 and 4. In any case, severe overlapping for the central GlcNAc units was observed and the conclusions should be regarded as semiquantitative. For both oligosaccharides, the pyranoid rings can be described as essentially monoconformational: $^4C_1$, as de-

duced from the vicinal proton proton couplings (data not shown). Then, NOESY and ROESY experiments were used to qualitatively estimate proton/proton inter-residue distances [25]. For **1**, all NOESY cross peaks were negative at 500 MHz and 299 K. The distance results estimated by using the isolated spin pair approximation are given in Table 2. Although only approximated, the Fuc H-1/H-2 intra-residue signals were used as reference (2.5 Å). Since overlapping is present, these data should be regarded as merely qualitative. Thus, the NOEs were assigned as strong (s), medium (m), and weak (w). The MD-calculated distances are shown in Table 2. It can be observed that a good matching is observed between the distances found experimentally and those estimated through molecular mechanics and dynamics simulations. The obtained results may indicate that, as least for

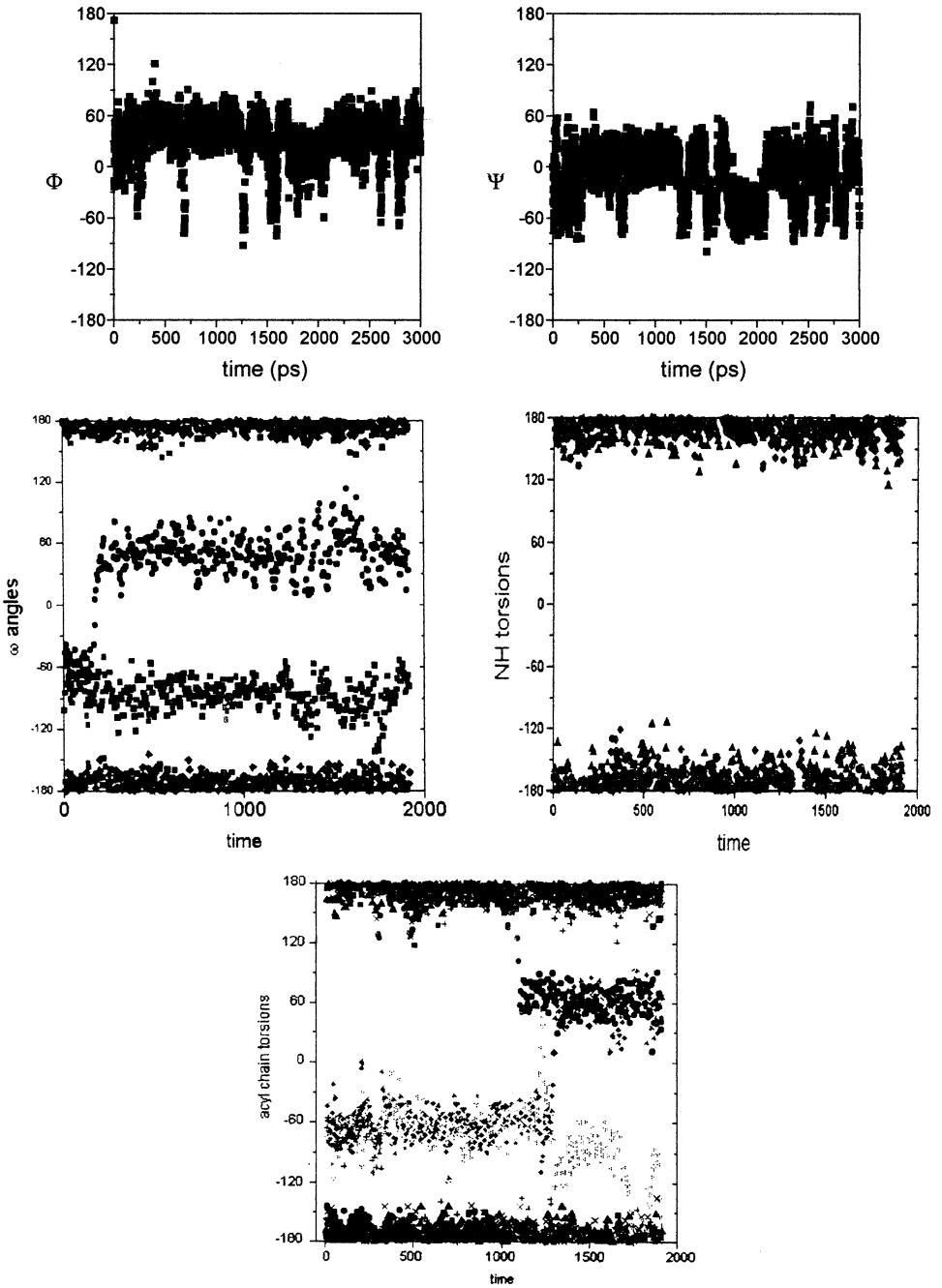

Fig. 5. Trajectory plots of the MD simulation (1 ns) of **2** by using MM3* (GB/SA). The Φ/Ψ histories of the simulation for one of the β(1→4) glycosidic linkage and the history of ω, NH, and lipid chain torsion angles are shown.

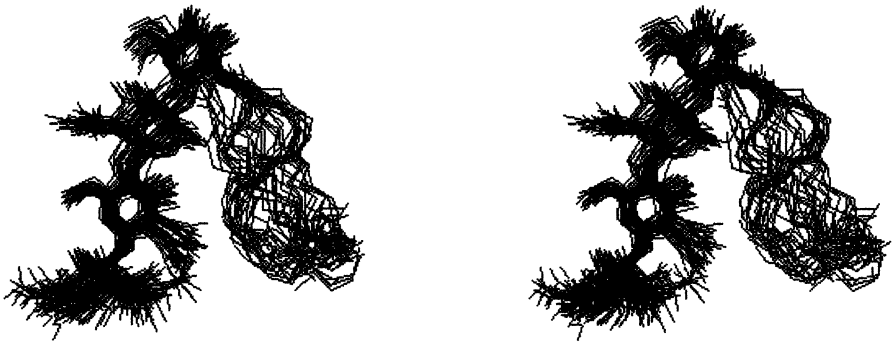

Fig. 6. Superimposition of several snapshots taken from the MD simulations of **2** (MM3*, GB/SA). The possibility of a quasi-parallel orientation of the acyl chain with respect to the oligosaccharide backbone has been emphasised.

Table 3
^{1}H NMR data (δ ppm) of **1** in DMSO-d_6 and of **2** in D_2O [a]

Ring	H1	H2	H3	H4	H5	H6S	H6R
A	4.91	3.28	3.66	3.46	3.79	1.04	3.37
B^{α}	4.85/5.19	3.58/3.74	3.76/3.94	3.46/3.70	3.60/4.09	3.46/4.25	3.59/4.12
B^{β}	4.41/4.72	3.44/3.73	3.44/3.72	3.36/3.72	3.36/3.74	3.28/4.17	3.35/4.12
C	4.35/4.56	3.48/3.78	3.23/3.58	3.22/3.61	3.29/3.71	3.28/3.88	3.59/3.71
D	4.35/4.56	3.48/3.78	3.23/3.52	3.22/3.61	3.29/3.71	3.36/3.86	3.61/3.68
E	4.32/4.60	3.43/3.82	3.24/3.58	3.01/3.49	3.15/3.50	3.69/3.94	3.35/3.77

[a] ^{1}H NMR signals for the lipid chain: (**1**) double bond, 5.31. CH_3 group, 0.84 ppm, amide linked –CH_2– 2.05 ppm, double bond linked –CH_2– 1.97 ppm, rest of the lipid chain, 1.16–1.30 ppm. NHAc groups, 1.76–1.82 ppm; (**2**) double bond, 5.44. CH_3 group, 0.88 ppm, amide linked –CH_2–, 2.30 ppm, double bond linked –CH_2–, 2.06 ppm, rest of the lipid chain, 1.28–1.35 ppm. NHAc groups, 2.03–2.08 ppm.

Table 4
^{13}C NMR data (δ ppm) of **1** in DMSO-d_6 and of **2** in D_2O [a]

A	96.5	78.0	68.6	72.4	65.6	16.0	58.0
B^{α}	91.0, 92.0	56.3, 54.4	68.1, 72.8	71.6, 79.2	68.6, 69.2	65.4, 66.8	–
B^{β}	101.5, 98.6	56.4, 55.6	72.4, 72.8	80.4, 79.2	80.4, 69.2	62.7, 66.8	–
C	101.5, 103.7	54.2, 56.0	74.4, 75.6	81.4, 80.0	81.0, 80.4	59.9, 60.8	–
D	101.5, 103.7	54.2, 56.0	74.4, 75.6	81.4, 80.0	81.0, 80.4	59.9, 60.8	–
E	103.0, 103.7	54.8, 55.4	74.4, 74.4	70.4, 71.2	76.5, 76.8	60.7, 61.6	–

[a] ^{13}C NMR signals for the lipid chain: (**1**) double bond: 130.0 ppm. CH_3 groups: 13.8 ppm, amide linked –CH_2–: 35.6 ppm, double bond linked –CH_2–: 26.5 ppm, rest of the lipid chain: 25.0, 29.0, 21.8, 28.3, 31.2 ppm. NHAc groups: 22.6 ppm. (**2**) double bond: 132.0 ppm. CH_3 groups: 14.8 ppm, amide linked –CH_2–: 36.8 ppm, double bond linked –CH_2–: 28.0 ppm, rest of the lipid chain: 26.4–29.6 ppm. NHAc groups: 24.3 ppm. CO groups: 173.2–173.8.

this particular case, these unrestrained MD simulations [26] provide a fair description of the motion around the different glycosidic linkages of this molecule. Regarding the acyl chain, no NOE contacts between its protons and those of the oligosaccharide, apart from the trivial ones with H-2 of the non-reducing end, were observed, probably indicating that this chain may adopt a variety of conformations.

Therefore summarizing the theoretical and experimental results, it seems that there is an important amount of conformational freedom for the glycosidic and exocyclic torsion angles of the lipopentasaccharide, although a representative major conformer may be deduced from Fig. 4.

For **2**, spectra were recorded in pure heavy water. NOESY cross peaks were again negative (Fig. 7) at 500 MHz and 299 K. The estimated interproton distances are given in

Table 3. Although only approximated, GlcNAc H-1/H-3 + 5 intra-residue signals were used as reference. Again, severe overlapping precludes a quantitative analysis, and the data should be regarded as merely qualitative. Thus, the NOEs were again catalogued as strong (s), medium (m), and weak (w). The MD-calculated distances are shown in Table 3. Basically, the results indicate a conformational behaviour for the oligosaccharide backbone, similar to that described above for the fucosyl derivative. Nevertheless, a major difference is observed regarding the acyl chain. In this case, strong NOE contacts among several fatty acid protons and those of the oligosaccharide are observed, indicating that, in water solution, the lipid chain may spend a significant amount of time adopting a quasi-parallel orientation to the oligosaccharide backbone (Fig. 6). The influence of the solvent in the conformational equilibrium of oligosaccharides has been documented [27]. In this case, although the conformational equilibrium around Φ/Ψ angles of the tetrasaccharide backbone is similar in both solvents, the major differences occur for the relative orientation of the lipid chain.

Therefore, summarizing the experimental results, it seems that there is an important amount of conformational freedom for the glycosidic and exocyclic torsion angles of the saccharides, with a major difference regarding

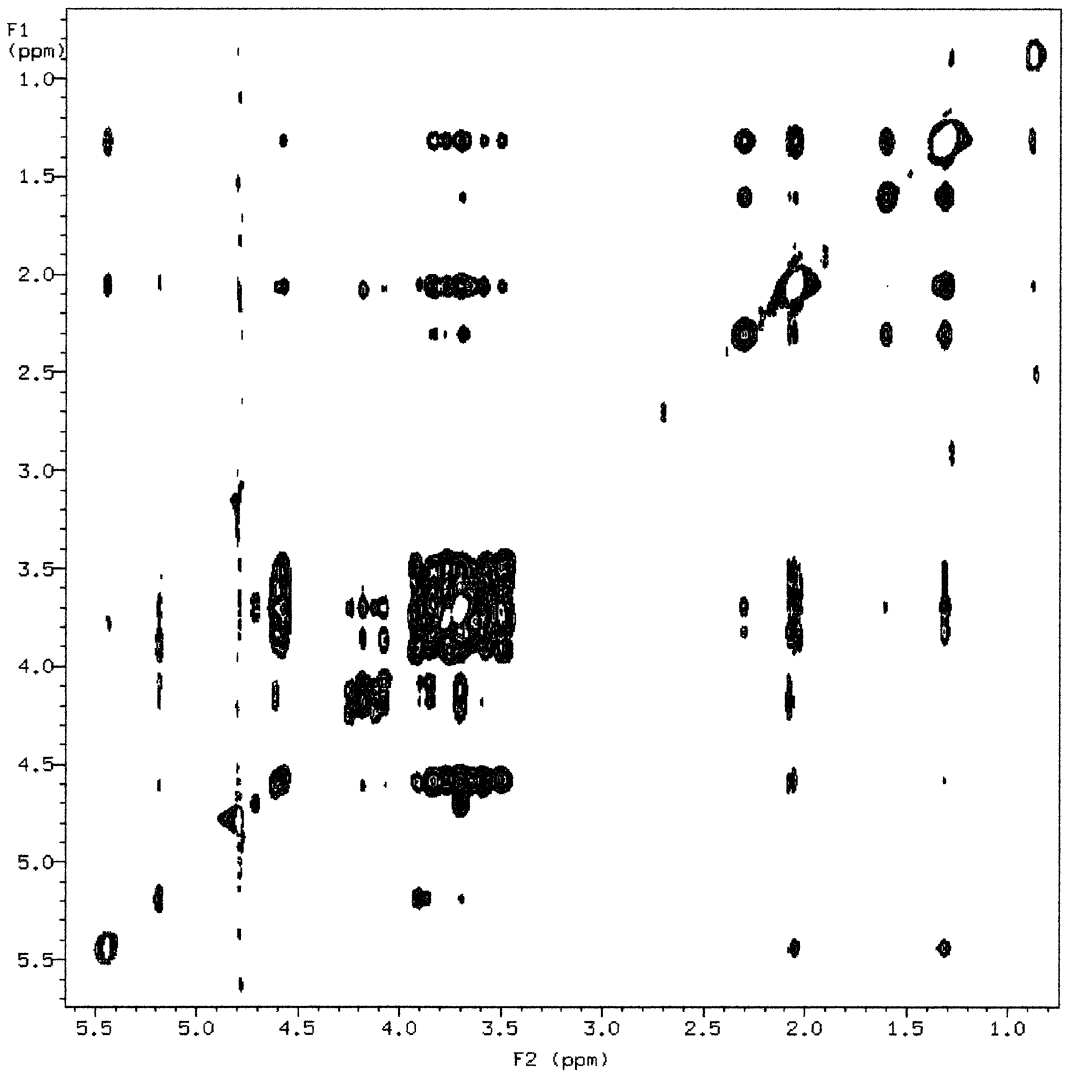

Fig. 7. NOESY 500 MHz spectrum of **2** (mixing time 300 ms) in D_2O solution. NOEs between the aliphatic protons of the acyl chain and the sugar residues are evident, indicating the existence of a quasi-parallel relative orientation of both moieties during a relevant fraction of time.

the orientation of the lipid chain. In water solution, there is a stabilization of conformers which present hydrophobic contacts between the sugar units and the fatty acid, while in a relatively less polar solvent such as DMSO, these contacts do not take place. It is clear from these data that the nature of the receptor binding site may modulate the conformational behaviour of the Nod factor, giving rise to different biological responses.

Acknowledgements

Financial support by DGICYT (Grants PB96-0833 and BIO96-1469-C03) is gratefully acknowledged. The authors also thank Dr J.E. Ruiz-Sainz (Departamento de Microbiología, Facultad de Biología, Universidad de Sevilla) for supplying bacterial cultures. L.G. would like to thank Ministerio de Educacion y Ciencia for a postdoctoral fellowship.

References

[1] J. Dénarié, F. Debellé, J.-C. Promé, *Ann. Rev. Biochem.*, 65 (1996) 503–535.
[2] R.W. Carlson, N.P.J. Price, G. Stacey, *Mol. Plant Microbe Interact.*, 7 (1995) 684–695.
[3] J.L. Firmin, K.E. Wilson, L. Rossen, A.W.B. Johnson, *Nature*, 324 (1986) 90–94.
[4] M.M.A. Olsthoorn, I.M. Lopez-Lara, B.O. Petersen, K. Bock, J. Haverkamp, H.P. Spaink, J.E. Thomas-Oates, *Biochemistry*, 37 (1998) 9024–9032.
[5] H.P. Spaink, G.V. Bloemberg, A.A.N. van Brussel, B.J.J. Lugtenberg, K.M.G.M. van der Drift, J. Haverkamp, J.E. Thomas-Oates, *Mol. Plant Microbe Interact.*, 8 (1995) 155–164.
[6] P. Roche, F. Debelle, F. Maillet, P. Lerouge, C. Faucher, G. Truchet, J. Denarié, J.-C. Promé, *Cell*, 67 (1991) 1131–1143.
[7] N.P.J. Price, F. Talmont, J.-M. Wieruszeski, D. Promé, J.-C. Promé, *Carbohydr. Res.*, 289 (1996) 115–136.
[8] R.W. Carlson, J. Sanjuan, U.R. Bath, J. Glushka, H.P. Spaink, A.H.M. Wijfjer, A.A.N. van Brussel, T.J.W. Stokkermans, K. Peters, G. Stacey, *J. Biol. Chem.*, 268 (1993) 18372–18381.
[9] M.P. Bec-Ferté, H.B. Krishnan, D. Promé, A. Savagnac, S.G. Pueppke, J.-C. Promé, *Biochemistry*, 33 (1994) 11782–11788.
[10] A.M. Gil-Serrano, G. Franco-Rodríguez, P. Tejero-Mateo, J. Thomas-Oates, H.P. Spaink, J.E. Ruiz-Sainz, M. Megías, Y. Lamrabet, *Carbohydr. Res.*, 303 (1997) 435–443.
[11] (a) K.C. Nicolaou, N.J. Bockovich, D.R. Carcanague, C.W. Hummel, L.F. Even, *J. Am. Chem. Soc.*, 114 (1992) 8701–8702. (b) L.X. Wang, C. Li, Q. Wang, Y.Z. Hui, *Tetrahedron Lett.*, 34 (1993) 7763–7766. (c) S. Ikeshita, A. Sakamoto, Y. Nakahara, Y. Kakahara, T. Ogawa, *Tetrahedron Lett.*, 35 (1994) 3123–3126. (d) D. Tailler, J.C. Jacquinet, J.M. Beau, *J. Chem. Soc., Chem. Commun.*, (1994) 1827–1828. (e) I. Robina, E. López-Barba, J. Jiménez-Barbero, M. Martín-Pastor, J. Fuentes *Tetrahedron Asymm.*, 8 (1997) 1207–1224. (f) L.X. Wang, C. Li, Q. Wang, Y.Z. Hui, *J. Chem. Soc., Perkin Trans 1*, (1994) 621–628. (g) J.S. Debenham, R. Rdebaugh, B. Fraser-Reid, *J. Org. Chem.*, 61 (1996) 6478–6479.
[12] I. Robina, E. López-Barba, J. Fuentes, *Tetrahedron*, 52 (1996) 10771–10784.
[13] N. Mantegazza, E. Samain, H. Driguez (to be published).
[14] A.T. Hagler, S. Lifson, P. Dauber, *J. Am. Chem. Soc.*, 101 (1979) 512.
[15] F. Mohamadi, N.G.I. Richards, W.C. Guida, R. Liskamp, C. Canfield, G. Chang, T. Hendrickson, W.C. Still, *J. Comput. Chem.*, 11 (1990) 440–467.
[16] K. Bock, J. Duus, *J. Carbohydr. Chem.*, 13 (1994) 513–543.
[17] W.C. Still, A. Tempczyk, R.C. Hawley, T. Hendrickson, *J. Am. Chem. Soc.*, 112 (1990) 6127–6128.
[18] A.D. French, J.D. Brady (Eds.). *Computer Modelling of Carbohydrate Molecules*, ACS Symp. Ser., 430, 1990.
[19] D. Lamba, S. Glover, W. Mackie, A. Rashid, B. Sheldrick, S. Perez, *Glycobiology*, 4 (1994) 151–163.
[20] (a) S.W. Homans, *Biochemistry*, 29 (1990) 9110–18. (b) B.J. Hardy, W. Egan, G. Widmalm, *Int. J. Biol. Macromol.*, 17–18 (1995) 149–60. (c) C.J. Edge, U.C. Singh, R. Bazzo, G.L. Taylor, R.A. Dwek, T.W. Rademacher, *Biochemistry*, 29 (1990) 1971–74. (d) P.J. Hajduk, D.A. Horita, L. Lerner, *J. Am. Chem. Soc.*, 115 (1993) 9196–201. (e) T.J. Rutherford, D.G. Spackman, P.J. Simpson, S.W. Homans, *Glycobiology*, 4 (1994) 59–68. (f) A. Poveda, J.L. Asensio, M. Martin-Pastor, J. Jimenez-Barbero, *J. Chem. Soc., Chem. Commun.*, (1996) 421–422.
[21] For a revision on the use of pulse field gradients in NMR, see J.T. Keeler, R.T. Clowes, A.L. Davies, E.D. Laue, *Methods Enzymol.*, 239 (1994) 145–207.
[22] (a) H.C. Siebert, G. Reuter, R. Schauer, C.W. von der Lieth, J. Dabrowski, *Biochemistry*, 31 (1992) 6962–6971. (b) J.L. Asensio, M. Martin–Pastor, J. Jimenez-Barbero, *Int. J. Biol. Macromol.*, 17 (1995) 52–55. (c) J.M. Coteron, K. Singh, J.L. Asensio, M.D. Dalda, A. Fernández-Mayoralas, J. Jiménez-Barbero, M. Martín-Lomas, *J. Org. Chem.*, 60 (1995) 1502–1513. (d) M.K. Dowd, P.J. Reilly, A.D. French, *J. Comput. Chem.*, 13 (1992) 102–114. (e) J.F. Espinosa, J.L. Asensio, M. Bruix, J. Jimenez-Barbero, *Ann. Quim. Int. Ed.*, 96 (1996) 320–324. (f) J.L. Asensio, M. Martin-Pastor, J. Jimenez-Barbero, *J. Mol. Struct.*, 395–396 (1997) 245–270.
[23] R.U. Lemieux, K. Bock, L.T.J. Delbaere, S. Koto, V.S. Rao, *Can. J. Chem.*, 58 (1980) 631–653.
[24] (a) J.P. Carver, *Pure Appl. Chem.*, 65 (1993) 763–770. (b) K. Bock, *Pure Appl. Chem.*, 55 (1983) 605–622.
[25] D. Neuhaus, M.P. Williamson, *The Nuclear Overhauser Effect in Structural and Conformational Analysis*, VCH, New York, 1989.
[26] (a) T.J. Rutherford, S.W. Homans, *Biochemistry*, 33 (1994) 9606–9614. (b) T.J. Rutherford, D.C.A. Neville, S.W. Homans, *Biochemistry*, 34 (1995) 14131–14137.
[27] (a) C.A. Bush, Z.-Y. Yan, B.N.N. Rao, *J. Am. Chem. Soc.*, 108 (1986) 6168–6173. (b) L. Poppe, C.W. von der Lieth, J. Dabrowski, *J. Am. Chem. Soc.*, 112 (1990) 7762–7771.